

Formation and properties of metal-oxygen atomic chains

W.H.A. Thijssen,¹ M. Strange,² J.M.J. aan de Brugh,^{2,3} and J.M. van Ruitenbeek¹

¹*Kamerlingh Onnes Laboratory, Leiden University,
P.O. Box 9504, 2300 RA Leiden, The Netherlands*

²*Center for Atomic-Scale Materials Physics, Department of Physics,
Technical University of Denmark, DK-2800 Lyngby, Denmark*

³*Solid State Physics Group, MESA+ Research Institute,
University of Twente, P.O. Box 217, 7500 AE Enschede, The Netherlands*

(Dated: November 4, 2021)

Suspended chains consisting of single noble metal and oxygen atoms have been formed. We provide evidence that oxygen can react with and be incorporated into metallic one-dimensional atomic chains. Oxygen incorporation reinforces the linear bonds in the chain, which facilitates the creation of longer atomic chains. The mechanical and electrical properties of these diatomic chains have been investigated by determining local vibration modes of the chain and by measuring the dependence of the average chain-conductance on the length of the chain. Additionally, we have performed calculations that give insight in the physical mechanism of the oxygen-induced strengthening of the linear bonds and the conductance of the metal-oxygen chains.

PACS numbers: 73.63.Rt, 73.40.Jn, 81.07.Lk, 68.35.-p

I. INTRODUCTION

Freely suspended atomically thin metallic wires are the ultimate one-dimensional conductors. Since their discovery^{1,2}, scientists have been amazed by the mere existence of these wires, since at first one would not expect such one-dimensional structures to be able to physically exist: The capillary instability that is also observed when droplets break off a forming water column would destroy the one-dimensionality since the surface tension is not strong enough to keep the structure together. In fact atomic wires are only observed when they are suspended between metal electrodes at both sides or supported by a substrate onto which they can be artificially be created atom by atoms^{3,4} or formed by self-assembly⁵. Once the wire breaks due to a critical built-up of stress in the chain, the atoms collapse back to the electrode since the necessary wire tension that kept the structure together has disappeared. Atomic wires have actually only been observed for the three 5d transition metals Au, Pt and Ir in break-junction experiments at low temperatures⁶. Although there has been an indication for the formation of short silver chains in TEM experiments at room temperature in UHV⁷. It has been argued that the physical mechanism that drives atomic chain formation is similar to what drives spontaneous surface reconstructions in these same metals, a delicate balance between the s and d electron density of states influenced by relativistic effects^{8,9}. Due to the high charge of the nucleus the lowest s-electron orbitals become relativistically contracted, which causes a lowering of the Fermi energy resulting in a small depletion of the anti-bonding states in the d-band. In the case of the 5d transition metals this relativistic effect is large enough to tip the energy balance for the formation of surface reconstructions and the formation of atomic chains. This is not the case for 4d and 3d transition metals⁶. Indeed a Ag(110) surface does form

a missing row reconstruction while Au(110) does.

Experimentally freely suspended atomic wires can be created by means of the mechanically controlled break junction (MCBJ) technique¹⁰, which is employed in this work. With this technique a small junction can be mechanically broken and be brought into contact again. Alternative approaches involve the use of a STM, the tip of which can be contacted with a surface¹¹ or by creating holes in a thin metallic foil by electron bombardment until a single strand of gold atoms is left, which can be imaged by TEM.^{2,12} The MCBJ technique and the electron bombardment technique have shown a large discrepancy in the observed interatomic distances between the atoms in the chain. For a gold chain created by the MCBJ technique in cryogenic vacuum an interatomic distance of $2.5 \pm 0.2 \text{ \AA}$ is observed¹³ while room temperature TEM images give distances up to 4 \AA ^{2,12}. Based on model calculations, it has been suggested that these large interatomic distances are due to the incorporation of foreign atoms like oxygen¹⁴, hydrogen¹⁵, carbon or nitrogen¹⁶ that are not resolved by TEM. Especially oxygen is an interesting candidate since Density Functional Theory (DFT) calculations have shown that the total energy of a gold atomic chain with atomic oxygen incorporated is lowered compared to clean gold¹⁴ and the Au-O bond is able to sustain higher pulling forces before breaking¹⁷. We have previously given experimental evidence showing that oxygen can indeed be incorporated into atomic gold chains and that oxygen induces chain formation for silver, which is known not to form chains in pure form¹⁸. In this article we will provide further evidence for oxygen incorporation by demonstrating the presence of oxygen in the chain by local vibration-mode spectroscopy and by calculations on the conductance properties of the chains, which strongly support our experimental observations.

II. EXPERIMENTAL TECHNIQUE

In our experiments we used poly-crystalline Au, Ag and Cu wires with a diameter of $100 \mu\text{m}$ and a purity of 99.999 %. After creating a circular notch in the middle of the wire, it is fixed on a bendable substrate in a three point bending configuration. By using a mechanical axle the wire can be broken and with a piezoelectric element it is possible to control the distance between the two electrodes with atomic precision. A detailed description of the MBCJ technique can be found in Ref 19. Our experiments were performed in cryogenic vacuum. Once the sample chamber is evacuated and cooled down to 5 K the wire is broken for the first time ensuring clean fracture surfaces. Close to the junction a local heater and thermometer are mounted, which enable us to control the temperature of the junction between 5 and 60 K, while the vacuum can remains at 5 K. In order to be able to admit oxygen to the junction the insert is equipped with a capillary attached to a high purity oxygen reservoir. To prevent premature condensation of oxygen, the capillary has a heating wire running all along the interior. To prevent other molecules to enter into the sample chamber while admitting oxygen through the heated capillary, it is pumped and baked out by means of the heating wire at $150 \text{ }^\circ\text{C}$, prior to the cool down. Two point conductance measurements are performed to determine the conductance of the atomic wires. Differential conductance (dI/dV) measurements were performed on the atomic wires using a lock-in amplifier. The bias voltage was modulated with a fixed modulation amplitude of 1 mV and a frequency of 7 kHz, while sweeping the dc bias voltage from + 100 mV to - 100 mV and back.

III. OBSERVATION OF OXYGEN INDUCED ATOMIC CHAINS

Microscopic junctions of gold, silver and copper are carefully broken and the conductance is observed to decrease stepwise until finally the contact has a cross section equal to the diameter of only a single atom. For the noble metals the conductance of single-atom contacts is close to one quantum unit of conductance, $G_0 = 2e^2/h$. For gold it is known that upon stretching a single atom contact, additional atoms can be pulled out of the electrodes to form a monatomic chain of up to 7 atoms long^{1,20,21}. This manifests itself in long plateaus with conductances around $1 G_0$ that are observed while monitoring the conductance of gold contacts as they are pulled apart. Such long plateaus are not observed for silver and copper as can be seen in Fig. 1. This indicates that silver and copper do not form long single atom wires like gold does.

When oxygen is admitted to the contact and the temperature is kept at 5 K, interesting differences in the conductances and lengths of the last plateaus are observed: In the case of gold the conductance and the av-

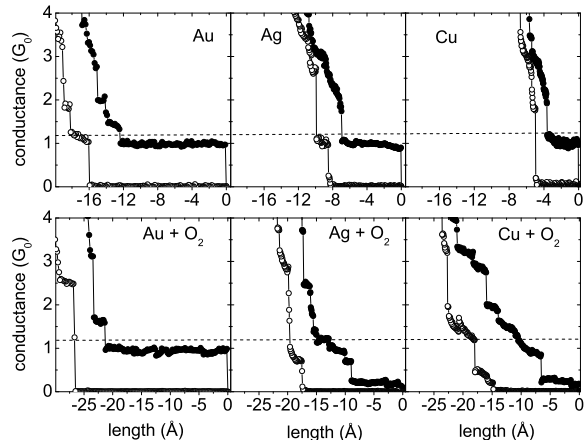


FIG. 1: Typical conductance traces for gold, silver and copper with and without oxygen admitted. The filled dots show the digitalized points measured while breaking the contact, while the open dots are measured when closing the junction again.

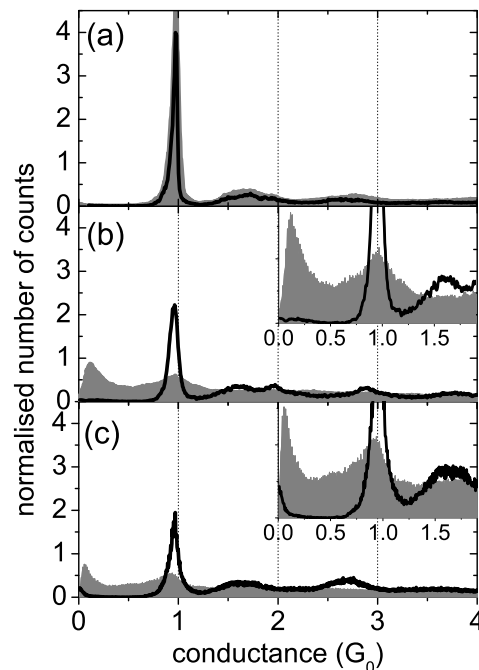


FIG. 2: Conductance histograms for Au (a), Ag (b) and Cu (c) without (black curves) and with oxygen admitted (filled graphs). For clarity the histograms have been normalized to the area under the curves. Each histogram is constructed from the digitalized points (filled dots of Fig. 1) obtained from approximately 2000 curves recorded at a bias voltage of 50 mV at $T = 5 \text{ K}$.

erage length of the chains does not change noticeably. This is in contrast to what is seen in the case of the non-chain-forming metals silver and copper. The con-

ductance of the last plateau drops sharply towards $0.1 G_0$ and $0.2 G_0$ for silver and copper, respectively, and the average total length increases dramatically. Only when the temperature of the gold sample is increased to about 40 K the average chain length also increases. One way to obtain more quantitative information about the conductance of the atomic contacts and chains is to record conductance histograms. By recording all conductances that are measured when a contact is being pulled apart and plotting them in a histogram a conductance histogram is obtained. After breaking and measuring many junctions the preferential conductances can be determined. In Fig. 2 conductance histograms for the three noble metals are shown with and without oxygen admitted. In order to focus on the changes that occur due to the admission of oxygen the histograms have been normalized to the area under the curves. For the clean metals one can clearly see that a peak near $1 G_0$ is dominant over all other conductances. When oxygen is introduced the dominant peak at $1 G_0$ decreases sharply for silver and copper due to a shift of weight to lower conductance values. For gold at 5 K no significant changes are seen as was discussed above. These observations indicate that oxygen influences the atomic contacts of silver and copper in such a way that configurations with conductances near $1 G_0$ are less frequently obtained. The conductance of atomic contacts for gold is apparently hardly influenced by oxygen since the conductance histograms of Fig. 2 are nearly identical.

Recently we have presented evidence¹⁸ that Au atomic wires become reinforced and therefore can be stretched to longer lengths as a result of their reaction with oxygen at 40 K. Furthermore, we have shown that this bond strengthening effect is even more pronounced for silver wires. We have studied the chain formation process under the influence of oxygen for the three noble metals. Since the conductance of an atomic chain or single-atom contact of noble metals are known to be close to $1 G_0$ we can measure the lengths of a large ensemble of conductance plateaus near $1 G_0$ and construct a length histogram. In such histogram the lengths of the plateaus are plotted against the number of times those lengths were observed. It can be clearly seen from the conductance histograms of Fig. 2 that in the case of silver and copper with oxygen admitted a large portion of the observed conductances have values below $1 G_0$. We suspect that these low conductance values belong to silver and copper atomic wires that are influenced by oxygen and therefore we have included these conductances in the chain length measurements. The length of the chains is obtained by measuring the distance, which the electrodes move apart from the moment when the conductance of the contact drops below $1.1 G_0$ until it drops below $0.05 G_0$. In the case of gold a conductance limit of $0.5 G_0$ was used for stopping the chain length measurement.

In Fig. 3 (a), (c) and (e) the length histograms for the three clean noble metals and those with oxygen admitted are shown. What is immediately seen is that the average chain length for all three metals increases upon

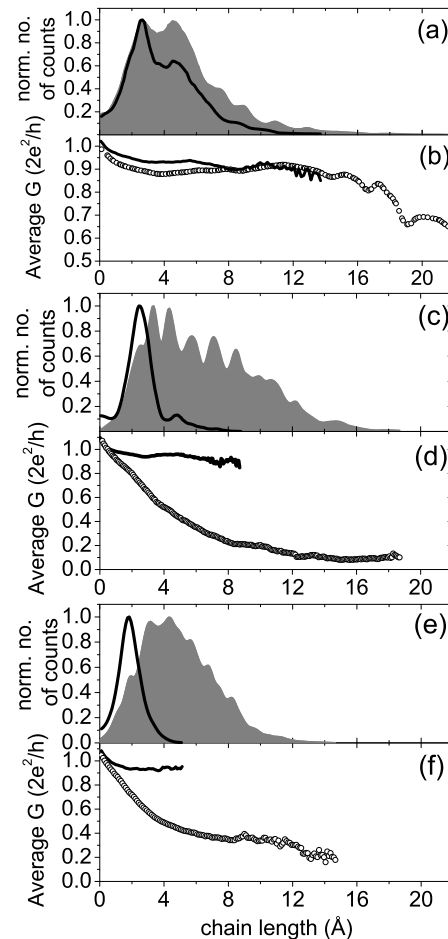


FIG. 3: Length histograms of stretch distances for contacts with conductance near $1 G_0$ and lower of Au (a), Ag (c) and Cu (e) in pure form (black curves) and with oxygen admitted (filled graphs). For the pure metals the lengths were measured in a conductance window of $G \in [1.1, 0.5]$, while with oxygen admitted $G \in [1.1, 0.05]$. The lower panels show the average conductance as a function of stretch distance for clean Au (b), Ag (d) and Cu (f) (black curves) and with oxygen admitted (open dots). All data were obtained with a bias voltage of 50 mV. The temperature graphs (a) and (b) was 40 K and for (c) to (f) 5 K.

oxygen admission. This effect is clearly the strongest for the non-chain-forming metals silver and copper. In all length histograms one can clearly see a number of more or less equidistant peaks. For silver-oxygen and copper-oxygen chains the distances between the peaks are about $1.5 \pm 0.2 \text{ \AA}$ and $1.2 \pm 0.2 \text{ \AA}$, respectively. These equidistant peaks give a strong indication of atomic chains being formed and the distances between the peaks have previously been interpreted as the interatomic distance in the chains¹. When assuming that oxygen is indeed taken up in the atomic chain structure, the interpretation of the peak structure in terms of bond lengths for such a di-

atomic chain is less straight forward. A bond length of only 1.2 Å is not expected and is about 60% smaller than for the gold-oxygen chains (see Fig. 3a). DFT calculations have predicted bond lengths of 1.9 Å and 1.8 Å for silver-oxygen and copper-oxygen chains respectively²². The shoulder to the left of the silver-oxygen length histogram of Fig. 3 is located at the same position as the dominant peak in the clean silver histogram. Therefore it is most probably caused by the rupture of a $>Ag-Ag<$ contact. Here we have introduced the notation $>$ and $<$ that indicate the connections to the left and right electrodes, respectively. We will take a more detailed look at the peak positions that arise in the length histograms of Fig. 3(c), in order to explain the discrepancy. A length count is taken at the moment an atomic chain breaks and the atoms collapse back to the electrodes, which causes the the conductance of the junction to drop deep into the tunneling regime. A rupture can occur when one of the linear one-dimensional bonds cannot be stretched any further due to a critical built-up of energy in the chain. But sometimes it is possible that an additional atom, which is weakly bound to the bulk atoms at one of the electrode apexes, is pulled into the atomic chain. Consequently, the chain remains intact and the tension of the linear bonds is relaxed. Then it is possible to stretch the one-dimensional structure further until again a critical built-up of energy occurs, which can result into rupture or the elongation of the chain with yet another atom. This sequence repeats itself over and over again and the incorporation of atoms will stop when the supply of loosely bound atoms at the apexes of the electrodes is depleted. The peaks in the length histograms indicate lengths at which there is a higher preference for the atomic chain to break and therefore represent atomic chain lengths in a stretched configuration.

In table I all peak positions together with an interpretation in terms of the corresponding chain composition are listed. From the length histogram of clean silver in Fig. 3 we obtain a silver-silver bond length of 2.4 Å and in order to simplify the analysis we kept this value fixed. Furthermore we assume that the bond length at the edges where the atomic chain is contacted to the electrodes with either a silver ($>Ag$) or an oxygen atom ($>O$) is the same. From this simple analysis we arrive at a silver-oxygen bond length of 1.8 ± 0.1 Å, very close to the theoretical value^{22,23}. A similar analysis can be made for the peak positions of the copper-oxygen length histogram of Fig. 3(e), which yields a copper-oxygen bond of 1.7 ± 0.1 Å.

The decrease of the conductance of the chains as the chains become longer is very nicely seen in Fig. 3 (b), (d) and (f). While for silver-oxygen and copper-oxygen chains the drop in conductance starts already for relatively short chains, gold-oxygen chains display a lower conductance only when they are on average longer than about 16 Å, corresponding to a chain with a length of more than six gold atoms. Indeed for Au-O chains created at 40 K it is sometimes observed that upon stretch-

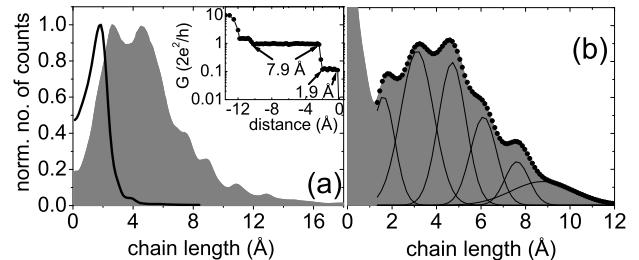


FIG. 4: (a) Length histogram for Au-O chains at 40 K with conductance limits between 1.1 and 0.5 G_0 (filled graph) compared to a length histogram with conductance limits between 0.2 and 0.05 G_0 (black curve); (b) Length histogram of Ag-O chains at 5 K with conductance values between 0.5 and 0.05 G_0 . All histogram were taken at a bias voltage of 50 mV and consist of at least 2000 traces.

ing the conductance makes as sudden jump from a value around 1 G_0 to about 0.1 G_0 as can be seen in the inset of Fig. 4(a). We have investigated these lower conduction plateaus by recording a length histogram between conductance values of 0.2 and 0.05 G_0 . In figure 4(a) the length histogram for low conductance values of Au-O chains is shown. It is dominated by a single peak at 1.9 Å. A second small peak can be seen at 3.9 Å. This distance is the same as the Au-O distance that we observed in the length histogram of Fig. 3(a). Furthermore it is striking that plateaus at 0.1 G_0 are typically only one bond length long and only occur when a chain of certain length has already been formed. We conclude, therefore, that the atomic unit that is being pulled into the chain

peak position (Å)	proposed chain compositions	number of Ag-O bonds	length of Ag-O bond
3.3	$>Ag-O-Ag<$ or $>O-Ag-O<$	2	1.7 Å
4.3	$>Ag-Ag-O<$	1	1.9 Å
5.7	$>Ag-Ag-O-Ag<$ $>Ag-O-Ag-O<$	2 3	1.7 Å 1.9 Å
7.1	$>Ag-O-Ag-O-Ag<$	4	1.8 Å
8.5	$>Ag-Ag-O-Ag-Ag<$ $>Ag-O-Ag-O-Ag-O<$	2 5	1.8 Å 1.7 Å
9.9	$>Ag-Ag-O-Ag-Ag-O<$ $>Ag-Ag-O-Ag-O-Ag<$	3 4	1.7 Å 1.9 Å
10.7	$>Ag-O-Ag-O-Ag-O-Ag<$	6	1.8 Å
12.2	$>Ag-Ag-O-Ag-O-Ag-Ag<$ $>Ag-O-Ag-O-Ag-O-Ag-O<$	4 7	1.9 Å 1.7 Å
14.8	$>Ag-Ag-O-Ag-O-Ag-O-Ag-Ag<$ $>Ag-O-Ag-O-Ag-O-Ag-O-Ag<$	6 8	1.7 Å 1.9 Å

TABLE I: Silver-oxygen chain configurations that fit the experimental peaks positions from the length histogram of figure 3(c). The numbers and lengths of the silver-oxygen bonds are also given.

and causes the sharp drop in conductance, also destabilizes the chain since upon further pulling the chain breaks in nearly all cases. The plateaus at $0.1 G_0$ have only been seen at temperatures ≥ 40 K. The higher mobility and vapor pressure of oxygen molecules at those temperatures increases the supply of oxygen molecules around the region where the chain is formed. We speculate that the low conductance plateau is caused by the appearance of oxygen-oxygen bonds in the chain which could severely lower both the conductance and the bond strength.

A length histogram obtained for low-conductance silver-oxygen chain structures is shown in Fig. 4(b). In contrast to gold (Fig. 4(a)) chain formation continues by incorporating more atomic units into the chain since multiple peaks in the length histogram are observed. The inter-peak distance is 1.5 ± 0.2 Å, which is the same as in the histogram of Fig. 3(c), indicating that both silver and oxygen atoms are being pulled into the chain.

More evidence to support that freely suspended long atomic wires are being formed of gold, silver and copper with chemisorbed oxygen incorporated comes from the dependence of the average return length on the chain length. When an atomic wire is formed, atoms are pulled

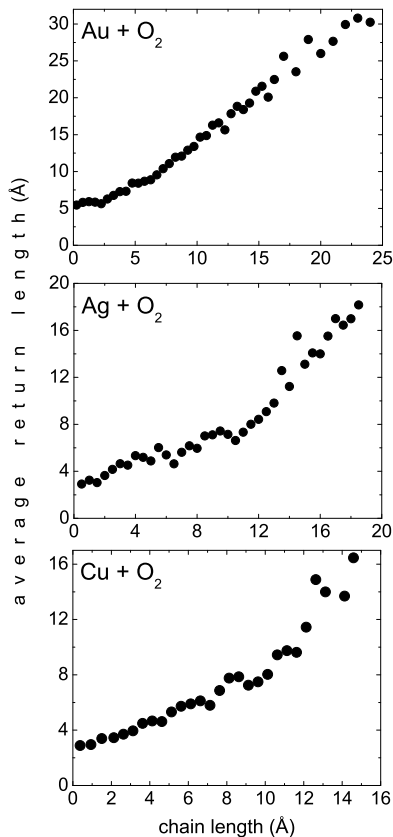


FIG. 5: Average return lengths as a function of atomic chain length for Au (a), Ag (b) and Cu (c) with admitted oxygen at respectively 40 K, 5 K and 5 K.

out of the electrodes in order to be incorporated into the atomic wire upon stretching the contact. When a wire breaks, the atoms collapse back to the electrodes and the conductance drops deep into the vacuum tunneling regime. We then reverse the direction of movement of the electrodes towards each other. At the moment that mechanical contact is remade the conductance jumps from a value in the tunneling regime to a value of order $1 G_0$. By measuring this so-called return length for every wire that is broken we obtain the average return length for a given atomic chain length. Fig. 5 shows the average return length for gold-oxygen, silver-oxygen and copper-oxygen chains. In all cases an offset is observed followed by an increase in average return length as a function of chain length. The offset indicates that even for a single atom contact that breaks before forming a chain the electrodes move back a certain distance. This is due to the fact that the single atom connects the two electrodes and it can sustain a force upon pulling on it. This causes a counterforce pulling on the electrodes, which will slightly elastically deform them. When the contact breaks the stress can be released and the atoms relax and move back into their equilibrium position. But when longer chains are being formed and eventually broken the atoms that made up the chain collapse back to the electrodes and consequently the electrodes have to move back a longer distance upon increasing chain length. Given the fact that the average return length increases more or less linearly with chain length we have a strong indication that atomic chains of noble metal atoms with oxygen are indeed being formed. The deviation from a purely linear increase can be the result of a larger energy stored in the longer chains, because more metal oxygen bonds are present that can sustain higher pulling forces. When such long chains break the stored elastic energy may propel atoms away from the junction area. The force a silver-oxygen bond in an infinite alternating silver-oxygen chain can sustain is about 2.4 times larger than for a silver-silver bond in a infinite silver chain²². While the difference in the case of pure gold and gold-oxygen is about a factor 1.5^{14,17} explaining why this effect is not appearing so clearly in gold-oxygen return lengths.

IV. POINT CONTACT SPECTROSCOPY ON METAL-OXYGEN CHAINS

In the previous section we have provided evidence that oxygen can chemically react with noble metal contacts or chains and reinforce the linear bonds in the wires so that they can be elongated further. In this section we present evidence that oxygen most probably is dissociated and incorporated into the atomic chains as is predicted by DFT model calculations^{14,17}.

We have verified the incorporation of oxygen by point contact spectroscopy. This technique forms a powerful tool for studying the interactions of electrons with vibrational excitations in a metallic contact^{24,25}. An atomic

chain of noble metal atoms is a ballistic conductor for low bias voltages, since it has one nearly completely transparent conduction channel resulting in a total conductance very close to $1 G_0$ ^{26,27,28}. However, electrons with sufficient energy have a small probability to excite phonon modes in an atomic chain and by means of differential conductance (dI/dV) spectroscopy the energies for those modes can be determined as was shown for clean gold atomic wires²⁹. About 1 % of all forward traveling electrons with an excess energy larger than the energy of a phonon mode actually do excite such mode. Those electrons lose energy, which forces them to scatter back since all forward moving states below $E_F + eV_{bias}$ are already occupied for a perfect single-channel conductor. This backscattering causes a small decrease of the total conductance of the atomic chain. The observation of this small signal is often hampered by conductance fluctuations, which result from interference of electron trajectories scattering off defects near the contact^{30,31}. In the case of the s-like noble metals that have a nearly 100% transparent single channel these conductance fluctuations are strongly suppressed³⁰. From Fig. 3 we see that gold-oxygen chains have a conductance that is close to $1 G_0$ and we have observed phonon modes for medium-length gold-oxygen wires. Differential conductance spectra were recorded by keeping the atomic chain at a fixed elongation and measuring the current modulation as was described before. Fig. 6 displays two spectra that were obtained for 7 Å long gold-oxygen wires at 5 K. Clearly two downward steps at different voltages in each spectrum can be seen, indicating a possible onset of phonon excitations at those energies. The low-energy phonon mode has an energy at 17 ± 2 meV in Fig. 6(a) and 15 ± 2 meV in Fig. 6(b). The high energy mode that is observed has an energy of 82 ± 4 meV and 60 ± 4 meV in Fig. 6(a) and Fig. 6(b) respectively. All spectra that we have observed, which display two phonon steps, have high energy modes between 60 and 80 meV.

In order to give a qualitative explanation of the observed vibration mode energies, let us take a look at a simple classical spring-mass model. The model consists of two gold atoms attached to solid walls and an oxygen atom connected by springs in between the gold atoms. We consider only the longitudinal eigenfrequencies, because the probability of exciting transversal modes is very small given the quasi one-dimensional geometry of the atomic chain. By solving the equations of motion we obtain three frequencies for masses M and m for gold and oxygen, respectively. Here we have used similar spring constants k between all masses for simplicity, and obtain

$$\begin{aligned} \omega_1^2 &= \frac{M+m-\sqrt{M^2+m^2}}{Mm} k \\ \omega_2^2 &= \frac{2}{M} k \\ \omega_3^2 &= \frac{M+m+\sqrt{M^2+m^2}}{Mm} k \end{aligned} \quad (1)$$

The lowest frequency mode ω_1 corresponds to the in-phase motion of all atoms. In the second mode ω_2 the

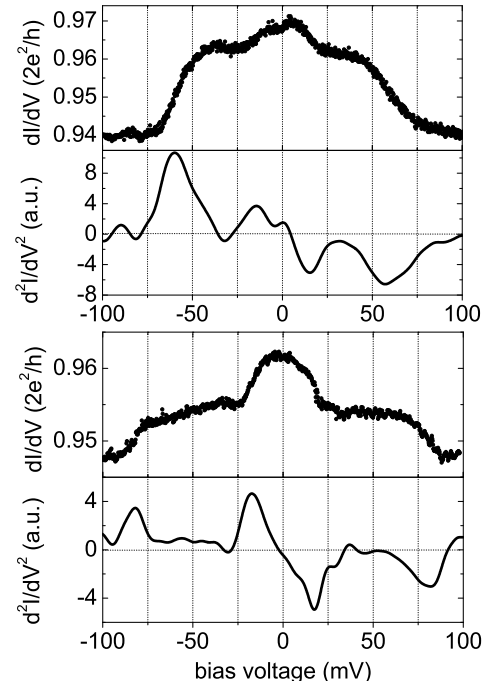


FIG. 6: Two typical differential conductance spectra taken for Au atomic chains after admitting oxygen at 4.2 K. The chains were pulled to a length of about 7 Å

oxygen atom is immobile and the gold atoms move in anti-phase. The highest frequency mode ω_3 corresponds to the oxygen atom moving in anti-phase with the gold atoms. By substituting the masses for gold and oxygen atoms, we find that the ratio of two low energy modes ω_1 and ω_2 is 1.4. The heavy-mass modes will be close to the energy of the longitudinal mode for clean atomic gold chains, that are found at about 10-15 meV depending on stretching²⁹. From Eq.(1) the high-energy mode can then be expected at 65 ± 10 meV. Preliminary DFT calculations on gold-oxygen chains predict a high energy mode in the range of 60 to 80 meV²³, depending on the stress in the linear bonds. Fig. 6 shows a high energy mode at 60 meV and one at 80 meV, comfortably in the range of our simple model and the preliminary calculations. Additionally, our analysis of the gold-oxygen vibration modes provides evidence that oxygen atoms, not molecules, are incorporated in the atomic chain: An oxygen molecule has double the mass of an atom, which would shift the energy of the vibration mode down by a factor $\sqrt{2}$ to 46 ± 7 meV, assuming a similar bond strength to gold, clearly off the experimental values.

We also performed point contact spectroscopy on silver-oxygen atomic chains. In contrast to the gold-oxygen atomic chains, the conductance of the silver-oxygen chains is typically much lower than $1 G_0$, which indicates that the conductance is not made up from a single fully transparent conduction channel. Normally,

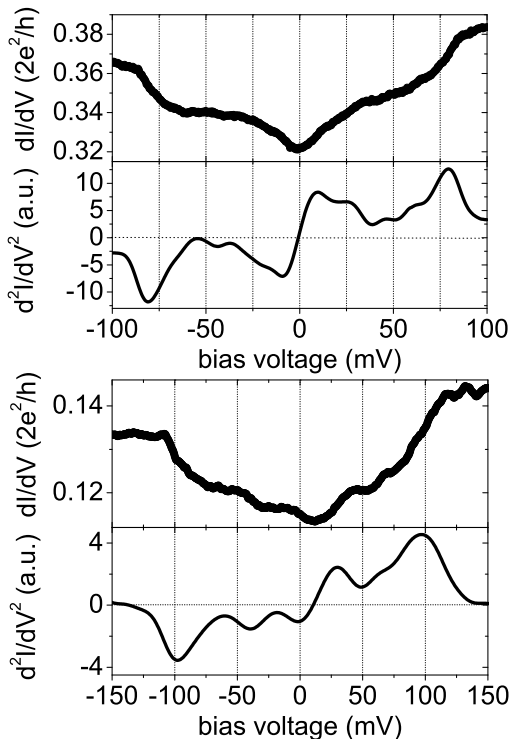


FIG. 7: Two dI/dV spectra taken for Ag atomic chains after admitting oxygen at 5 K. The top spectrum was obtained for a chain of about 7 Å in length and the bottom graph for a 11 Å long chain. The d^2I/dV^2 spectra have been smoothed for clarity.

when one deals with one or more partly opened conduction channels the dI/dV spectrum is dominated by conductance fluctuations³¹. This makes the observation of steps in dI/dV due to inelastic scattering of electrons on local vibration-modes very difficult. Furthermore it was recently claimed that the inelastic correction to the conductance changes from a negative contribution for a single conduction channel with $G > 0.5 G_0$ to positive for $G < 0.5 G_0$ ^{32,33,34}. We obtained a few spectra for silver-oxygen chains with a conductance $\leq 0.5 G_0$, which displayed bias-symmetric step-like features at energies far above 20 meV (see Fig. 7).

One can distinguish clearly a step-like increase of the conductance around 80 and 100 meV for the top and bottom spectra, respectively, which would indicate forward scattered inelastic electrons, in agreement with theory³⁴. The energies of 80-100 meV are in the range where local vibration modes of these one-dimensional structures can be expected, albeit that compared to the 60-80 meV for the gold-oxygen chains they are somewhat high. Since the energy is far above the Debye energy for silver, the modes are related to incorporated oxygen in the chain.

V. CALCULATIONS

In this section we present DFT calculations for the conductance, bonding properties and vibrational properties of Ag-O contacts. Electronic structure calculations are performed using a plane wave implementation of DFT.³⁵ Exchange and correlation effects are treated at the GGA level using the PW91 energy functional³⁶ and the nuclei and core electrons are described by ultrasoft pseudopotentials.³⁷ The Kohn Sham (KS) eigenstates are expanded in plane waves with a kinetic energy less than 400 eV. The width of the Fermi-Dirac distribution for occupation numbers is set to 0.1 eV and the total energies are extrapolated to $T = 0$.

We first consider a linear Ag chain with an interatomic distance of 2.6 Å and a linear alternating Ag-O chain with an interatomic distance of 2.0 Å. The supercell for the chains has transverse dimensions $12\text{Å} \times 12\text{Å}$ and we align the chains to the z -direction.

The band structure for Ag and Ag-O chains are shown in Fig. 8 in the upper and lower graph, respectively. The dashed lines indicate slightly strained chains, with the

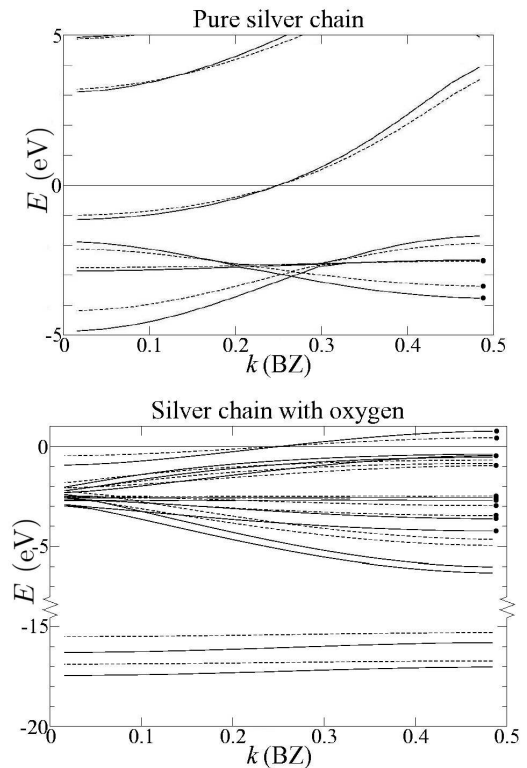


FIG. 8: Upper graph: Band structure for an infinite pure silver chain with an interatomic distance of 2.6 Å (continuous lines) and 2.8 Å (dashed lines). No spin polarization. Lower graph: Band structure of an infinite alternating silver-oxygen chain with an interatomic distance of 2.0 Å (continuous lines) and 2.2 Å (dashed lines). Bands are split in spin up and spin down bands and degenerate bands are marked with a dot. In both cases, 32 k -points are used for the whole Brillouin zone.

interatomic distance increased by 0.2 Å.

The Ag chain is not magnetic and has fully occupied 4d bands and a half filled 5s band. For the Ag-O chain we find a magnetic moment of $1.0 \mu_B$ per Ag-O atom unit and the energy gain, due to the spin-polarization is 0.12 eV per Ag-O atom unit.

The bands for the Ag-O chain can be grouped according to the angular momentum quanta, m , in the chain direction. The two lowest lying bands are the spin-split O $2s$ ($m=0$) bands. The remaining bands shown are Ag $4d$ bands ($m = \pm 2$) and Ag $4d - O 2p$ hybrid bands ($m = 0, \pm 1$). Straining the Ag-O chain changes the profile of all bands (dashed lines). However, only two of the spin bands with $d - p$ character change considerably indicating that these bands are relevant for the covalent bonding between Ag and O. The two bands are singly degenerate since they have $m=0$ and corresponds to a $d_{z^2} - p_z$ hybrid band with bonding character. Novaes *et. al*¹⁷ recently showed that the covalent bond between Au and O is mainly due to the bonding state between Au $5d_{z^2}$ and O $2p_z$, in agreement with our findings. It has been argued before that an interesting connection exists between the observation of surface reconstructions and the atomic chain formation in the metals gold, platinum and iridium.⁶ In this context it is remarkable that oxygen induced surface reconstructions on Ag(110) and Cu(110) have been observed,^{39,40} while we here provide experimental evidence for atomic chain formation for these metals upon oxygen chemisorption. Therefore we suspect that the oxygen chemisorption on metal surfaces and the consequent reconstruction originates from the $d - p$ hybrid bands playing the same role as the d -bands in the chain forming metals.

There is a doubly degenerate spin band crossing the Fermi level in Fig. 8 with $m = \pm 1$, i.e. a $d_{xy} - p_x$ band and a $d_{yz} - p_y$ band. This shows, that magnetic Ag-O chains are metallic and can support two spin channels for a total maximum conductance of $1 G_0$. However, our experiments show, that finite Ag-O chains often display conductances considerably below $1 G_0$ conductances.

To investigate this, we have calculated the spin-paired transmission function for finite Ag-O wires with semi-infinite silver chains as leads. For comparison we have also performed calculations with gold instead of silver. We use a Green's function method for phase coherent electron transport, where both the Green's function of the semi-infinite leads and the scattering region are evaluated in terms of basis consisting of maximally localized Wannier functions.³⁸

Fig. 9 (a) and (b), show the transmission functions for finite Ag-O and Au-O wires sandwiched between Ag and Au chains, respectively. The full line is for a $>Ag/Au-O<$ wire sandwiched between leads and the dashed line is for $>Ag/Au-O-Ag/Au-O<$ wire between the leads. The Fermi level is at zero and indicated by the vertical dashed line.

The transmission function for $>Ag-O<$ displays one eigenchannel in the energy range -2 eV to 3 eV, indi-

catating that the eigenchannel state has $m = 0$. The only available state on the O atom with $m = 0$ in the relevant energy range is the $2p_z$, which is then the current carrying state on the O atom. This is confirmed by the projected density of states for O $2p_z$ (not shown), showing the resonance in the transmission function below the Fermi level originating from an anti-bonding combination of the O $2p_z$ orbital and the Ag d_{z^2} band in the leads. The broadening of the resonance is due to the coupling to the s-band in Ag. The bonding combination falls outside the Ag lead bands and is a bound state. In the case of $>Ag-O-Ag-O<$ units, the two resonances have a similar origin, but the transmission at the Fermi level is reduced considerably.

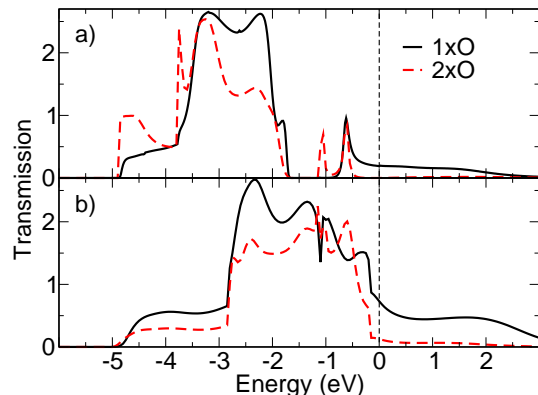


FIG. 9: (a) Transmission function for a $>Ag-O<$ (full curve) and $>Ag-O-Ag-O<$ (dashed curve) wire contacted by semi-infinite silver atomic wires. (b) Transmission function for a $>Au-O<$ (full curve) and $>Au-O-Au-O<$ (dashed curve) wire contacted by semi-infinite gold atomic wires.

The transmission function for the Au-O system shown in Fig. 9 (b) consists of single eigenchannel with $m=0$, in the energy range from -0.15 eV to 3.0 eV. Below -0.15 eV, there are Au d -bands with $m = \pm 1$ which can couple to O $m = \pm 1$ states. This results in two extra eigenchannels making the $2p_z$ resonance less visible except for the tail starting at -0.15 eV and extending to 3 eV.

As seen in Fig.9 (a) and (b) an oxygen atom scatters more strongly electrons around the Fermi level in the $m = 0$ channel in the case of Ag than for Au. This is in agreement with our experiments, as we observed in Fig.3 a tendency for Ag-O chains to have a lower conductance than Au-O chains. However, in a more realistic contact with surface electrodes as leads, we suspect a finite coupling between $m = \pm 1$ finite $d - 2p$ hybrid chain states and the d states in the metal electrodes, which would result in a higher conductance. A conductance calculation on Ag-O chains involving more realistic electrodes will be published elsewhere.

We also studied the longitudinal vibration-mode energies of a single oxygen atom in a silver contact, we define a supercell with 3×3 atoms in the surface plane and which contains 7 atomic layers. The oxygen atom is

clamped between two 4 atom pyramids pointing in opposite directions and is attached to Ag (111) surfaces. The Ag (111) surfaces are separated by 12.7 Å. We use a 4×4 k-point Monkhorstpack mesh in the surface Brillouin zone. The two pyramids and the oxygen atom, were relaxed, until the total residual force was below 0.05 eV/Å. The calculated longitudinal vibrational mode energies for the two apex silver atoms and the oxygen atom are: $\omega_1 = 81.4$ meV, $\omega_2 = 28.5$ meV and $\omega_3 = 14.7$ meV. The 3 vibrational modes corresponds to: 1) The oxygen atom moving in anti-phase with the silver atoms. 2) The two Ag atoms moving in anti-phase and the oxygen atom being immobile. 3) In phase motion of all 3 atoms.

The relation between the vibration-mode energies can be accounted for by a simple model as described in the previous section and we indeed see that the value of the calculated high energy mode is in good agreement, with the measured vibrational energies in the range (80 – 100) meV, indicating that single oxygen atoms are indeed incorporated in the chains.

Recently Ishida⁴¹ presented calculations for chains of Au and Ag atoms with a single O atom inserted. Ishida's results also show a high transmission at the Fermi energy for oxygen in Au chains, although for a single O atom it has more the character of a resonance. For Ag the conductance is more strongly suppressed.

VI. CONCLUSION

We have studied the effects of oxygen on the atomic chain formation for the noble metals gold, silver and

copper. By studying the conductance and mechanical properties of these atomic chains, we provided evidence that oxygen atoms can be incorporated in atomic chains. While atomic gold chains retain a conductance near $1 G_0$ when oxygen is incorporated, the conductance is much reduced for silver and copper chains that form upon chemisorption of oxygen atoms. The increased linear bond strength makes it possible to form silver-oxygen and copper-oxygen atomic chains. Our analysis of the inter-atomic distances in the silver-oxygen and copper-oxygen chains has indicated the presence of metal-oxygen bonds in the chain. The point contact spectra obtained on the metal-oxygen chains give additional evidence that atomic (not molecular) oxygen is incorporated in the atomic chains. The observation that oxygen can be incorporated in atomic chains and thereby increasing the linear bond strength could open possibilities for other molecules to be incorporated in atomic chains. This could lead to interesting new physical properties of these ultimate one-dimensional structures.

This work is part of the research program of the "Stichting FOM," which is financially supported by NWO.

-
- ¹ A.I. Yanson, G. Rubio Bollinger, H.E. van den Brom, N. Agraït, and J.M. van Ruitenbeek, *Nature* **395**, 783 (1998).
² H. Ohnishi, Y. Kondo, and K. Takayanagi, *Nature* **395**, 780 (1998).
³ N. Nilius, T.M. Wallis and W. Ho, *Science* **297**, 1853 (2002).
⁴ T.M. Wallis, N. Nilius and W. Ho, *Phys. Rev. Lett.* **89**, 236802 (2002).
⁵ O. Gurlu, O. A. O. Adam, H.J. W. Zandvliet, and B. Poelsema, *Appl. Phys. Lett.* **83**, 4610 (2003).
⁶ R.H.M. Smit, C. Untiedt, A.I. Yanson, and J.M. van Ruitenbeek, *Phys. Rev. Lett.* **87**, 266102 (2001).
⁷ V. Rodrigues, J. Bettini, A.R. Rocha, L.G.C. Rego and D. Ugarte, *Phys. Rev. B* **65**, 153402 (2002).
⁸ N. Takeuchi, C.T. Chan and K.M. Ho, *Phys. Rev. Lett.* **63**, 1273 (1989); *Phys. Rev. B* **43**, 14363 (1991).
⁹ P. Pyykkö, *Chem. Rev.* **88**, 563 (1988).
¹⁰ C.J. Muller, J.M. van Ruitenbeek and L.J. de Jongh, *Phys. Rev. Lett.* **69**, 140 (1992).
¹¹ N. Agraït, J.G. Rodrigo and S. Vieira, *Phys. Rev. B* **47**, R12345 (1993).
¹² V. Rodrigues and D. Ugarte, *Phys. Rev.* **63**, 073405 (2001).
¹³ C. Untiedt, A.I. Yanson, R. Grande, G. Rubio Bollinger, N. Agraït, S. Vieira and J.M. van Ruitenbeek, *Phys. Rev. B* **66**, 085418 (2002).
¹⁴ S.R. Bahn, N. Lopez, J.K. Nørskov, and K.W. Jacobsen, *Phys. Rev. B* **66**, 081405 (2002).
¹⁵ N.V. Skorodumova and S.I. Simak, *Phys. Rev. B* **67**, 121404(R) (2003).
¹⁶ F.D. Novaes, A.J.R. da Silva, E.Z. da Silva and A. Fazzio, *Phys. Rev. Lett.* **90**, 036101 (2003).
¹⁷ F.D. Novaes, A.J.R. da Silva, E.Z. da Silva and A. Fazzio, *Phys. Rev. Lett.* **96**, 016104 (2006).
¹⁸ W.H.A. Thijssen, D. Marjenburgh, R.H. Bremmer and J.M. van Ruitenbeek, *Phys. Rev. Lett.* **96**, 026806 (2006).
¹⁹ N. Agraït, A. Levy Yeyati and J.M. van Ruitenbeek, *Phys. Rep.* **377**, 81 (2003).
²⁰ H. Hakkinen, R.N. Barnett, A.G. Scherbakov and U. Landman, *J. Chem. Phys. B* **104**, 9063 (2000).
²¹ S.R. Bahn and K.W. Jacobsen, *Phys. Rev. Lett.* **87**, 266101 (2001).
²² J.M.J. Aan de Brugh, Master Thesis, Technical University of Denmark (2005).
²³ A.J.R. da Silva, *private communication*.
²⁴ I.K. Yanson and O.I. Shklyarevskii, *Sov. J. Low Temp. Phys.* **12**, 509 (1986).
²⁵ A.V. Khotkevich and I.K. Yanson, *Atlas of Point Contact Spectra of Electron-phonon Interactions in Metals* (Kluwer

- Academic, Dordrecht, 1995).
- ²⁶ E. Scheer, N. Agraït, J.C. Cuevas, A. Levy Yeyati, B. Ludoph, A. Martín-Rodero, G. Rubio Bollinger, J.M. van Ruitenbeek and C. Urbina, *Nature* **394**, 154 (1998).
- ²⁷ H.E. van den Brom and J.M. van Ruitenbeek, *Phys. Rev. Lett.* **82**, 1526 (1999).
- ²⁸ E. Scheer, W. Belzig, Y. Naveh, M.H. Devoret, D. Esteve and C. Urbina, *Phys. Rev. Lett.* **86**, 284 (2001).
- ²⁹ N. Agraït, C. Untiedt, G. Rubio Bollinger, and S. Vieira, *Phys. Rev. Lett.* **88**, 216803 (2002).
- ³⁰ B. Ludoph, M.H. Devoret, D. Esteve, C. Urbina and J.M. van Ruitenbeek, *Phys. Rev. Lett.* **82**, 1530 (1999).
- ³¹ B. Ludoph and J.M. van Ruitenbeek, *Phys. Rev. B* **61**, 2273 (2000).
- ³² J.K. Viljas, J.C. Cuevas, F. Pauly and M. Häfner, *Phys. Rev. B* **72**, 245415 (2005).
- ³³ M. Paulsson, T. Frederiksen and M. Brandbyge, *Phys. Rev. B* **72**, 201101(R) (2005).
- ³⁴ L. de la Vega, A. Martín-Rodero, N. Agraït and A. Levy Yeyati, *Phys. Rev. B* **73**, 075428 (2006).
- ³⁵ W. Kohn and L. J. Sham, *Phys. Rev.* **140**, A1133 (1965).
- ³⁶ J. P. Perdew, J. A. Chevary, S. H. Vosko, K. A. Jackson, M. R. Pederson, D. J. Singh, and C. Fiolhais, *Phys. Rev. B* **46**, 6671 (1992).
- ³⁷ D. Vanderbilt, *Phys. Rev. B* **41**, R7892 (1990).
- ³⁸ K. S. Thygesen and K. W. Jacobsen, *Chem. Phys.* **319**, 111 (2006)
- ³⁹ M. Taniguchi, K. Tanaka, T. Hashizume, and T. Sakurai, *Surf. Sci. Lett.* **262**, L123 (1992).
- ⁴⁰ F. Besenbacher and J. K. Nørskov, *Progr. Surf. Sci* **44**, 5 (1993).
- ⁴¹ H. Ishida, *Phys. Rev. B* **75**, 205419 (2007).